NUMERICAL SIMULATION OF THE MIXING AND FLOW CHARACTERISTICS IN LOBED MIXERS

Zhi-Wu WANG [a*], Kun ZHANG [a], Longxi ZHENG [a], Xing-Gu CHEN [a], Ping LI [b], and Xiang-Yi NAN [b]

[a] School of Power and Energy, Northwestern Polytechnical University, Xi´an, China
[b] Xi´an Aerospace Propulsion Institute, Xi´an, China

Original scientific paper
DOI: 10.2298/TSCI120529140Z

This paper focused on the mixer optimization by numerical simulation. The mixing and flow characteristics inside two different lobed mixers with/without centrum were obtained by 3-D CFD simulation. The core flow was the hot rich-methane/O_2(1)burnt gas, while the cold air flew by the by-pass. The air/burnt gas flow ratio was improved from 7 to 9 in order to confirm the effect of air/burnt gas ratio on the mixing and flow characteristics. The simulation results indicated that no matter which mixer was used, there were a pair of symmetrical re-circulation regions in the mixers, and the total temperature and species distribution turned to be more uniform at the increased mixing length. The mixing performance in the lobed mixer with centrum was slightly better than that of the lobed mixer without centrum, and the length of re-circulation region in the lobed mixer with centrum was slightly shorter than that of the lobed mixer without centrum. The air/burnt gas ratio had considerable effect on the mixing and flow characteristics. The mixing performance with air/burnt gas ratio of 9 was much better than that of air/burnt gas ratio 7. Similar mixing performance would attain in the case of air/burnt gas ratio 9 with only half of the mixing length in the case of air/burnt gas ratio 7. The re-circulation region in the case of air/burnt gas ratio 9 occurred ahead of that of air/burnt gas ratio 7, and the former was longer than the latter.

Key words: *lobed mixer, mixing, afterburner, air/burnt gas ratio*

Introduction

In order to increase the cruising range and the accelerating ability of aircraft the afterburner with medium by-pass ratio should be equipped. When afterburner is designed, it is essential to make comprehensive design on the mixer, diffuser, flame holder, and fuel system. If the poor-oxygen burnt gas and air mix and combust fully in a very short length, the length of the afterburning chamber and the structural mass will decrease. Therefore, the engine performance is directly affected by the mixing and combusting of the gas and the air in the afterburner. In order to improve the combustion efficiency of the afterburner and even the engine performance, it is necessary to organize a good mixing and combustion process in the afterburner, and improve the mixing performance of the afterburner [1, 2].

Several mixers are classified by the structure as following: ring mixer, funnel shaped mixer, chrysanthemum shaped mixer (lobed mixer), and finger shaped mixer, *etc*. Nowadays,

* Corresponding author; e-mail: malsoo@mail.nwpu.edu.cn

the lobed mixer is used widely in the turbofan engine in the world, and ring mixer is used in some engines, especially in the low bypass ratio engine which is developed in recent years.

The mixing of two fluids could be strengthened by the lobed mixer, which performance had been found in the 1960 and used to reduce the noise of a turbofan engine. Later, further studies showed that the lobed mixer could improve the thrust of the engine, reduce the fuel consumption rate and restrain the infrared radiation of the aircraft exhaust system. Moreover, it also could be used to reduce the noise when the supersonic aircraft took off and landed, and strengthen the mixing of fuel and air in the burner and so on [3]. Thus, after 1980, the mixing mechanism of lobed mixer was investigated by experiment and numerical simulation, and some important results were achieved [4-11].

Assumed that the gas did not burn, the flow field formed by mixing the high temperature gas and the cold air was simulated to study the flow and mixing characteristics. A lobed mixer with inner penetration angle of 0 was designed in this paper. The influencing rule of air/burn gas ratio on the lobed mixer flow and mixing characteristics was studied by the full three-dimensional cold flow simulation, which provided some theoretical guidance for mixer selection and thermal performance study of the afterburner.

Physical model and computation method

Physical model

The equivalent diameter of the by-pass and the core flow is 155 mm and 94 mm, respectively. The axial length of the lobed mixer is 500 mm.

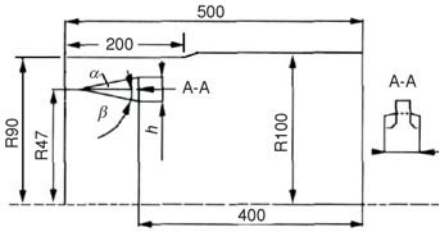

Figure 1. Schematic illustration of lobed mixer

The schematic illustration of the lobed mixer is shown in fig. 1, wherein the outer ring diameter of the lobe is 120 mm, the axial length of the lobe is 50 mm, the outer (α) and inner (β) penetration angles of the lobe are 34.21° and 0°, and the lobed mixer is divided into 8 lobes. The maximum radius of the by-pass is 100 mm, the entrance radius of core flow is 47 mm, the length from the lobe tail edge to the outlet of the mixer is 400 mm. The mixers were classified as two types: one was the lobed mixer with centrum, the other was the lobed mixer without centrum. Due to the complexity of the 3-D lobe model, unstructured mesh was used for grid division in the computational domain. Prism boundary mesh refinement of five layers was used for the lobed wall and the casing wall, and local mesh refinement was used for adjacent domain of the outlet of the lobes. The final mesh division is shown in fig. 2.

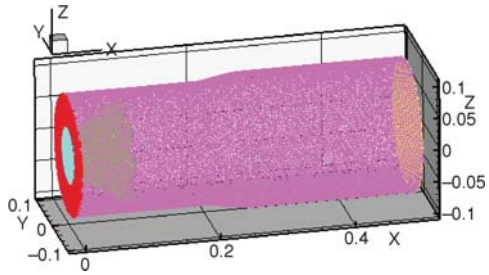

Figure 2. Computation field of lobed mixer

Computation method and boundary conditions

The mixing process of the gas and the air in the mixer is a complex flow process, which includes flow, mixing, and heat transfer process, *etc*. The commercial software FLUENT was used to study the flow and mixing characteristics of the lobed mixer in this paper. Standard wall

function was selected for the near wall. Second order upwind scheme was used to discrete the convective term in the flow equation. The first-order upwind scheme was used to discrete the terms in the other equations. SIMPLE algorithm was used for the coupling of flow and pressure.

Table 1. Boundary conditions

	P [MPa]	T [K]	Ma	$\dot{m}$ [kgs^{-1}]
Burnt gas of inner flow passage	0.22	910	0.3	0.643/0.5
Air of bypass	0.22	379	0.3	4.5

The burnt gas from core flow was methane/O_2 (l) burnt gas, while air flew by the by-pass. Due to the low flow velocity and small Mach number of the core and by-pass flow, the gases were treated as the incompressible gases. The velocity inlet boundary conditions were used to deal with the inlets of the inner flow passage and the bypass. The pressure outflow boundary condition was selected to deal with the outlet of the mixer. The solid wall boundary conditions were selected to deal with the lobed walls and the inside casing walls. The inlet parameters of the computational operating conditions were shown in tab.1, where P, T, Ma, and $\dot{m}$ represented the inlet total pressure, total temperature, Mach number, and mass flow rate, respectively.

The computation results and analysis

Lobed mixer without centrum

Figure 3 showed the velocity vector at the outlet section of the lobed mixer without centrum. It was seen from fig. 3 that the core flow over the lobe inner surface was directed upward to the lobe peak, and the by-pass flow over the lobe outer surface was directed downward to the lobe valley. An array of counter-rotating stream-wise vortices was formed at the trailing edge of the lobe, which was consistent with the computational result by Yong [6], as shown in fig. 4. The stream-wise vortices played an important role to mix the core and by-pass flow.

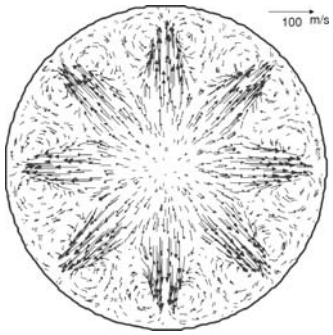

Figure 3. Velocity vector at the outlet section of the lobed mixer without centrum with air/burnt gas ratio of 7

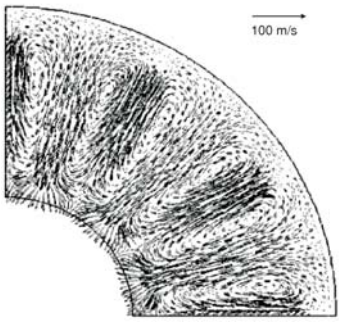

Figure 4. Velocity vector at the outlet section of the lobed mixer [6]

The contour figures of total temperature and CH_4 mass fraction at planes $z = 0$ and $x =$ 50, 100, 250, 400, and 490 of the lobed mixer without centrum with the air/burnt gas ratio of 7, were shown in figs. 5 and 6, respectively.

As shown in fig. 5, after the gases flew through the lobed, the burnt gas and the air mixed drastically, and the temperature near the mixer axis decreased sharply while the tempera-

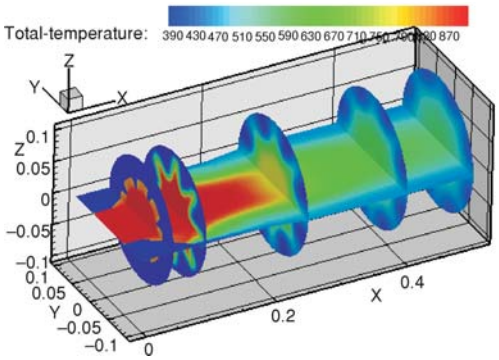

Figure 5. Contour figure of total temperature in the lobed mixer without centrum with air/burnt gas ratio of 7

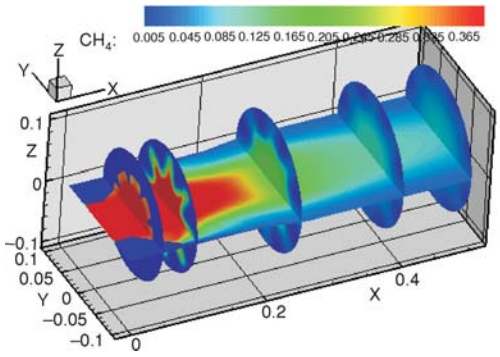

Figure 6. Contour figure of CH_4 mass fraction in the lobed mixer without centrum with air/burnt gas ratio of 7

ture near the mixer wall rose quickly. The high temperature region and maximum temperature decreased gradually with the continual mixing. The temperature distribution at planes x = 100, 250, 400, and 490 were different, in which the high temperature region corresponded to the flow passage of the high temperature gas in the lobes. The differences between the temperature near the mixer axis and near the mixer wall at plane z = 0 where near the mixer outlet were very small, which meant that the temperature distribution was uniform.

As shown in fig. 6, along with the mixing length, the mass fraction of CH_4 nearby the axis decreased gradually, while the mass fraction of CH_4 nearby the wall increased gradually. The distribution of the mass fraction of CH_4 turned to be uniform. The CH_4 distribution at planes x = 100, 250, 400, and 490 were slightly worse than that of plane z = 0, in which the regions of high mass fraction corresponded to the flow passage of the high temperature gas in the lobes.

Total temperature and CH_4 distributions at the intersection lines of the planes x = 100, 250, 400, and 490 with plane z = 0 were shownin fig. 7 and fig. 8, respectively . It could be seen clearly that the total temperature and mass fraction of CH4 near the axis decreased gradually as

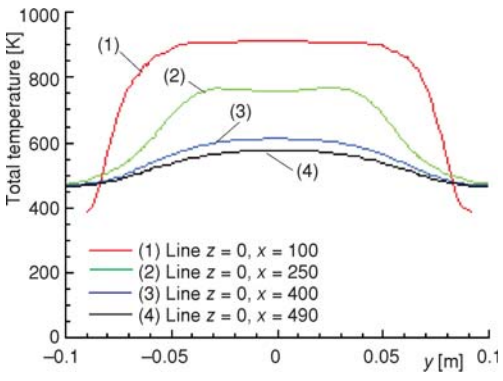

Figure 7. Total temperature distributions at the intersection lines of planes x = 100, 250, 400, and 490 with plane z = 0 without centrum with the air/burnt gas ratio of 7

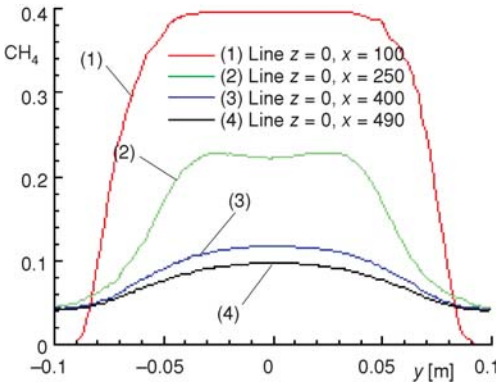

Figure 8. CH_4 mass fraction distributions at the intersection lines of planes x = 100, 250, 400, and 490 with plane z = 0 without centrum with the air/burnt gas ratio of 7

the mixing continued, while the temperature and mass fraction of CH_4 near the mixer wall increased gradually, the total temperature distribution and the CH_4 distribution turned to be uniform. At the intersection line of plane $x = 100$ with plane $z = 0$, the total temperature was still about 380 K and the mass fraction of CH_4 was still 0 near the mixer wall, which meant that the region near the mixer wall was not been affected by the mixing. However at the intersection line of plane $x = 250$ with plane $z = 0$, the total temperature increased to about 470 K and the mass fraction of CH_4 reached about 0.04 near the wall. The total temperature and the mass fraction of CH_4 distributions were very uniform before the outlet of mixer. At the intersection line of plane $x = 490$ with plane $z = 0$, the maximum total temperature nearby the mixer axis was about 570 K, and the minimum total temperature near the mixer wall was about 470 K. Meanwhile, the maximum mass fraction of CH_4 nearby the mixer axis was about 0.09, and the minimum mass fraction of CH_4 near the mixer wall was about 0.042.

The velocity vector figures at plane $z = 0$ of the lobed mixer without centrum with the air/burnt gas ratios of 7 and 9 were shown in fig. 9. Due to the temperature of the burnt gas was higher than that of the air, the velocity of the burnt gas was higher than that of the air, although the mach numbers of the burnt gas and air were the same. Behind the lobes, the burnt gas and the air mixed acutely, and the velocity of the core flow decreased. As shown in fig. 9(a), when air/burnt gas ratio was 7, a pair of symmetrical re-circulation zones occurred near the plane $x = 190$ and ended near the plane $x = 360$. When the air/burnt gas ratio increased to 9, a pair of symmetrical re-circulation zones occurred near the plane $x = 120$ and also ended near the plane

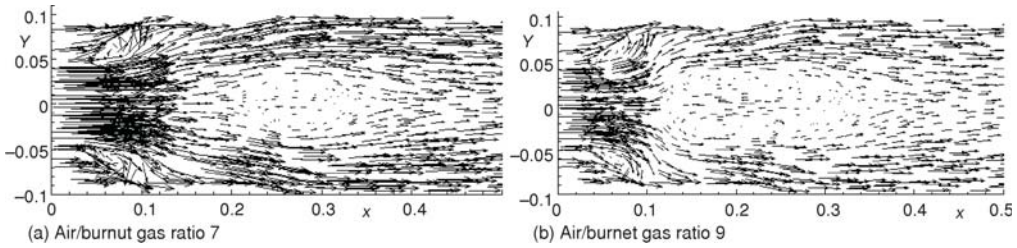

Figure 9. Velocity vector figures at $z = 0$ of the lobed mixer without centrum

$x = 360$, as shown in fig. 9(b). The re-circulation zones with low velocity were of benefit to ignition and combustion in the afterburner. When the air/burnt gas ratio was 9, the re-circulation zones formed earlier, the length of the re-circulation zones was longer, and the velocity distribution at the mixer outlet was more uniform than that of the air/burnt gas ratio 7.

Figures 10 and 11 showed, respectively, the distributions of the total temperature and the mass fraction of CH_4 at the intersection lines of planes $x = 100$, 250, 400, and 490 with plane $z = 0$ in the lobed mixer without centrum with the air/burnt gas ratio of 9. Compared with figs. 7 and 8, the distribution of the total temperature

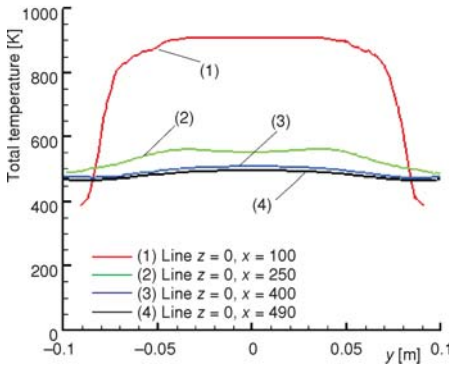

Figure 10. Total temperature distributions at the intersection lines of planes $x = 100$, 250, 400, and 490 with plane $z = 0$ without centrum with the air/burnt gas ratio of 9

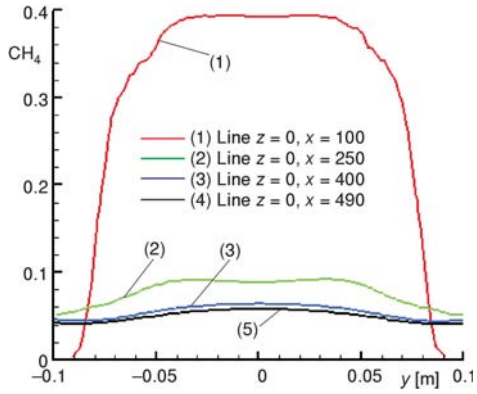

Figure 11. CH_4 mass fraction distributions at the intersection lines of planes x = 100, 250, 400, and 490 with plane z = 0 without centrum with the air/burnt gas ratio of 9

and CH_4 were basically the same at the intersection line of plane x = 100 with plane z = 0. However, the distributions of the total temperature and CH_4 at other three intersection lines were different, and the distributions of the total temperature and CH_4 with the air/burnt gas ratio of 9 were more uniform than that of ratio air/burnt gas ratio 7. The distributions of the total temperature and CH_4 at the intersection line of plane x = 250 with plane z = 0, when the air/burnt gas ratio was 9, were nearly the same with that of the intersection line of plane x = 490 with plane z = 0 when the air/burnt gas ratio was 7. At the intersection line of plane x = 490 with plane z = = 0, the maximum total temperature was about 495 K and the minimum total temperature was about 465 K, while the maximum mass fraction of CH_4 was 0.058 and the minimum was 0.041, which meant that the distribution of the total temperature and the distribution of the CH_4 mass fraction were uniform. Compared with the case of the air/burnt gas ratio of 7, the mixing performance was much better and the similar distributions of the total temperature and CH_4 fraction could form with just half of the mixing length in the case of air/burnt gas ratio of 9, which was beneficial to shorten the length of the combustion chamber. It was mainly because that when the length of the mixer was constant, the increase of the air/burnt gas ratio meant that the increase of the velocity ratio of the air/fuel (increased from 0.48 to 0.64), which enhanced the mixing.

Lobed mixer with centrum

The velocity vector figures at plane z = 0 of the lobed mixer with centrum with the air/burnt gas ratios of 7 and 9 were shown in fig. 12. The flow characteristics of the lobed mixer with centrum were similar to that of the lobed mixer without centrum and the velocity of the burnt gas (from core flow) was higher than the velocity of the air (from the bypass). Behind the lobes, the burnt gas and the air mixed acutely, and the velocity of core flow decreased. When the air/burnt gas ratio was 7, a pair of symmetrical re-circulation regions began to form near the plane x = 160, and ended near the plane x = 350. When the air/burnt gas ratio increased to 9, a pair of symmetrical re-circulation regions began to form near the plane x = 120, and also ended near the plane x = 350. When the air/burnt gas ratio was 9, the re-circulation zone formed earlier

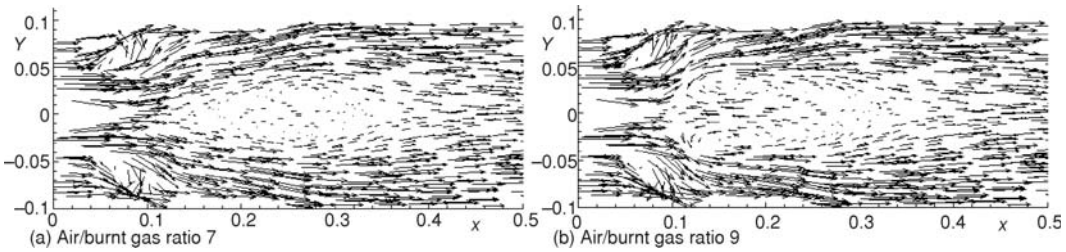

Figure 12. Velocity vector figures at plane z = 0 in the lobed mixer with centrum

and the length of the re-circulation zone was longer, meantime the velocity distribution at the mixer outlet was more uniform than that of air/burnt gas ratio of 7. The length of re-circulation zone in the lobed mixer with centrum was slightly shorter than that of lobed mixer without centrum.

The contour figures of total temperature and CH_4 mass fraction at planes $z = 0$ and $x = 50$, 100, 250, 400, and 490 of the lobed mixer with centrum, when the air/burnt gas ratio was 7, were shown in figs. 13 and 14, respectively. It could be seen that the change rules of the total temperature and CH_4 of the lobed mixer with centrum was similar to that of the lobed mixer without centrum. After the gases flew through the lobes, the burnt gas and the air mixed acutely, the temperature near the mixer axis decreased sharply while the temperature near the mixer wall rose quickly. The high temperature region and maximum temperature decreased gradually as the mixing continued. The differences between the temperature near the mixer axis and the temperature near the mixer wall at plane $z = 0$ near the mixer outlet decreased, in which the total temperature near the mixer axis was about 585 K, the temperature near the mixer wall was about 475 K, and the temperature distribution was relatively uniform.

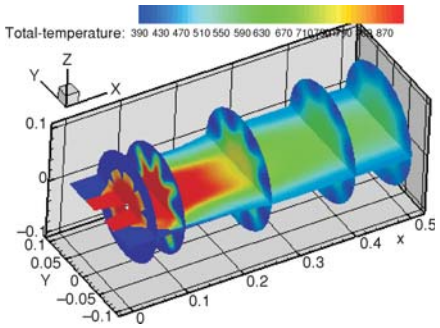

Figure 13. Contour figure of total temperature in the lobed mixer with centrum with air/burnt gas ratio of 7

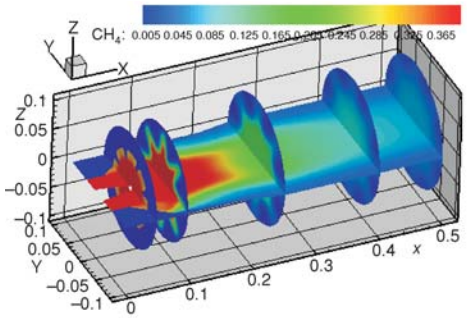

Figure 14. Contour figure of CH_4 mass fraction in the lobed mixer with centrum with air/burnt gas ratio of 7

The contour figures of total temperature and CH_4 mass fraction at planes $z = 0$ and $x = 50$, 100, 250, 400, and 490 of the lobed mixer with centrum, when the air/burnt gas ratio was 9, were shown in figs. 15 and 16, respectively.

In the area at the plane $z = 0$ and after the plane $x = 250$, there was a little difference between the temperature near the mixer axis and the temperature near the mixer wall, in which the temperature near the mixer wall was about 500 K, and the maximum temperature near the axis was about 544 K. At plane $x = 250$, the difference of temperature distribution was slightly big, in which the high temperature region corresponding to the flow passage of the high tem-

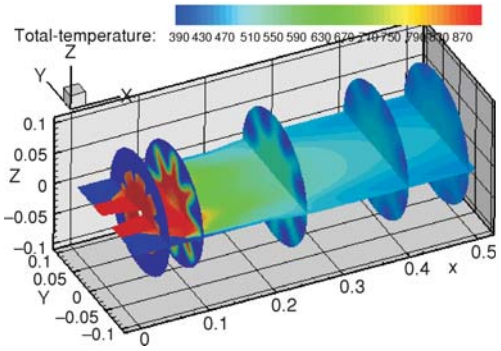

Figure 15. Contour figure of total temperature in the lobed mixer with centrum with air/burnt gas ratio of 9

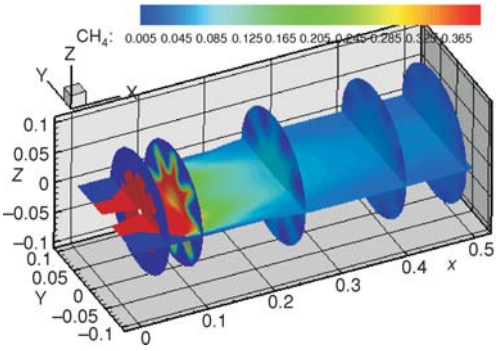

Figure 16. Contour figure of CH_4 mass fraction in the lobed mixer with centrum with air/burnt gas ratio of 9

perature burnt gas in the lobes. Behind the plane $x = 300$, the difference between the temperature near axis and the temperature near the mixer wall decreased further, in which the total temperature near the mixer axis was about 520 K, the temperature near the mixer wall was about 490 K, and the temperature distribution was much more uniform.

According to fig. 16, in the area at the plane $z = 0$ and after the plane $x = 250$, there was a little difference of mass fraction of CH_4 between that near the mixer wall and near the mixer axis, in which the mass fraction of CH_4 near the wall was about 0.059, and the maximum mass fraction of CH_4 near the axis was about 0.09, which meant that the CH_4 distribution with the air/burnt gas ratio of 9 was much uniform than that of ratio air/burnt gas ratio 7. But at plane $x = 250$, the difference of CH_4 distribution was slightly big, in which the region of high mass fraction of CH_4 corresponded to the flow passage of the high temperature burnt gas in the lobes. Behind plane $x = 300$, the difference between the mass fraction of CH_4 near the mixer wall and the mixer axis decreased further, in which the maximum mass fraction of CH_4 near the axis was about 0.074, and the mass fraction of CH_4 near the wall was about 0.055. Compared with the case of the air/burnt gas ratio of 7, the CH_4 mass fraction near the wall decreased from 0.059 to 0.055.

Similar to that of the lobed mixer without centrum, the mixing performance of the lobed mixer with centrum with air/burnt gas ratio of 9 was better than that of air/burnt gas ratio 7 and the similar distribution of temperature and CH_4 mass fraction could form with only half of the mixing length.

Figures 17 and 18 showed the distribution of the total temperature and the CH_4 mass fraction at the intersection line of planes $x = 100$, 250, 400, and 490 with plane $z = 0$ in the

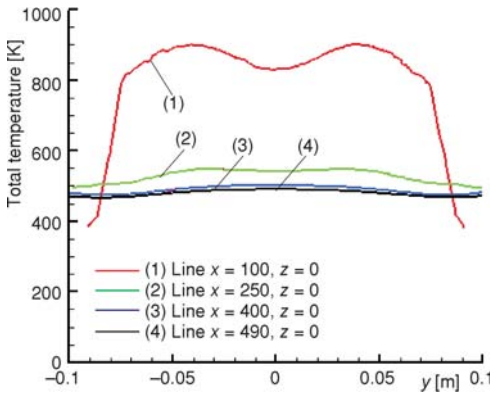

Figure 17. Total temperature distributions at the intersection line of plane $x = 100$, 250, 400, and 490 with plane $z = 0$ with centrum with the air/burnt gas ratio of 9

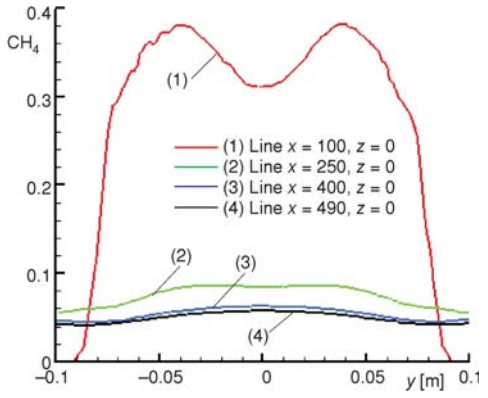

Figure 18. CH_4 mass fraction distributions at the intersection line of plane $x = 100$, 250, 400, and 490 with plane $z = 0$ with centrum with the air/burnt gas ratio of 9

lobed mixer with centrum when the air/burnt gas ratio was 9, respectively. Compared with figs. 10 and 11, the distributions of total temperature and CH_4 mass fraction at the intersection line of plane $x = 100$ with plane $z = 0$ were basically the same, while the distributions of total temperature and CH_4 mass fraction at other three lines were slightly uniform.

Table 2 showed the total temperature and mass fraction of CH_4 at the intersection line of plane $x = 490$ with plane $z = 0$ with different mixers. It was clearly seen from tab. 2 that the mixing performance in the lobed mixer with centrum was better than that of a lobed mixer without centrum, and the mixing performance in the case of air/burnt gas ratio of 9 was better than that of the air/burnt gas ratio of 9.

Table 2. The total temperature and CH_4 mass fraction at line $z = 0/x = 490$ with different mixers

	Lobed mixer without centrum		Lobed mixer with centrum	
	Air/burnt gas ratio of 7	Air/burnt gas ratio of 9	Air/burnt gas ratio of 7	Air/burnt gas ratio of 9
Average total temperature [K]	529	481	528	478
Minimal total temperature [K]	464	468	467	470
Maximum total temperature [K]	584	495	580	490
Average CH_4	0.0723	0.05	0.0448	0.0491
Minimal CH_4	0.041	0.0415	0.0404	0.0426
Maximum CH_4	0.0974	0.0579	0.081	0.0573

Conclusions

According to the 3-D CFD simulation of the lobed mixers with rich-methane/O_2(1) burnt gas and air, the main results was as follows.

- As the mixing of the burnt gas/ air in the mixers continued, the total temperature and the mass fraction of CH_4 near the mixer axis decrease gradually, while the total temperature and the mass fraction of CH_4 near the mixer wall increased gradually, and the distributions of the total temperature and the species mass fraction turned to be uniform.
- The mixing performance in the lobed mixer with centrum was slightly better than that of the lobed mixer without centrum.
- As the air/burnt gas ratio increased, the mixing performance improved. Similar mixing performance would attain in the case of air/burnt gas ratio of 9 with only half of the mixing length in the case of air/burnt gas ratio of 7, which was beneficial to shorten the length of the afterburner.

Acknowledgments

This work was supported by the National Natural Science Foundation of China through Grant No. (51306153), the Natural Science Foundation of Shanxi Province of China (grant number 2010JQ7005), Doctoral Fund of Ministry of Education of China (grant number 20116102120027) and NPU Foundation for Fundamental Research (grant number NPU-FFR-JCY20130129).

References

[1] Hou, X., *et al*., Combustion Technology for High Performance Aviation Gas Turbine [M] (in Chinese), Industry of National Defense University, Beijing, 2001
[2] Smith, L. L., *et al*., Mixing Enhancement in a Lobed Injector, *Physics Fluids 9*, (1997), 3, pp. 667- 678
[3] Liu, Y., Xie, L., Analytical Solution of Mixing Efficiency of Lobed Mixer (in Chinese), *Journal of Aerospace Power, 24* (2009), 4, pp. 740-745
[4] Liu, Y., *et al*., Effect of Cut Angles at Trailing Edge on the Performance of a Lobed Mixer (in Chinese), *Journal of Aerospace Power, 24* (2009), 9, pp. 1917-1922
[5] Lu Y., *et al*., Aerodynamic Performance of Lobed Mixers at Different Velocity Ratios (in Chinese), *Journal of Aerospace Power, 17* (2002), 1, pp. 53-57
[6] Shan, Y., *et al*., Numerical Investigation of Aerodynamic and Mixing Characteristics of Scarfed Lobed Mixer for Turbofan Engine Exhaust System, *Transactions of Nanjing University of Aeronautics & Astronautics, 26* (2009), 2, pp. 130-136
[7] Wu, C., *et al*., Mixer Investigation of Turbofan Engine with Pulse Detonation Afterburners (in Chinese), *Journal of Engineering Thermophysic, 30* (2009), 8, pp. 1437-1439
[8] Shan, Y., Zhang J., Numerical Investigation on the Effects of Lobe Nozzle Geometric Parameters on Mixer-Ejector Performance (in Chinese), *Journal of Aerospace Power, 20* (2005), 6, pp. 73-977
[9] Hu, C., *et al*., Effects of the Air Inlet Angle and Jet Number on Mixing Flow in the Afterburning Chamber of Solid Rocket Ramjet (in Chinese), J*ournal of Solid Rocket Technology, 26* (2003), 4, pp. 14-17
[10] Hui, H., *et al*., Mixing Process in a Lobed Jet Flow, *AIAA Journal, 40* (2002), 7, pp. 1339-1345
[11] Bridges J., Wernet, M. P., Cross-Stream PIV Measurements of Jets with Internal Lobed Mixers, AIAA 2004-2896, 10th AIAA/CEAS Aeroacoustics Conference, Manchester, UK, 2004

Paper submitted: May 29, 2013
Paper revised: August 3, 2013
Paper accepted: October 8, 2013